JOURNAL GEOLOGICAL SOCIETY OF INDIA
Vol.91, April 2018, pp.449-456

Induced and Ambient Crustal Seismicity under the Ghawar Oil-Gas Fields, Saudi Arabia

Manoj Mukhopadhyay[1*], Eslam Elawadi[1], Basab Mukhopadhyay[2] and Saad Mogren[1]

[1] King Saud University, P.O. Box 2455, Riyadh 11451, Saudi Arabia
[2] Geological Survey of India, 29 J.L. Nehru Road, Kolkata - 700 016, India
***E-mail:** mtrondhem@gmail.com*

ABSTRACT

The Ghawar anticline (GA) is the super-giant anticline belonging to a set of giant anticlines called the Rayn anticlines (RA) developed in the Eastern Province (EP), Saudi Arabia. The RA is situated within the Arabian block microplate forming the distant foreland of the Zagros. For the first time, using the *'Reviewed ISC Earthquake Catalogue'* for the period of 1970-2010, it is demonstrated that the EP crust is seismogenic down to a depth of ~15 km or more and has a typical surface width of ~220 km; this width is ostensibly six-times wider than that of GA. The Saudi Geological Survey (SGS) Earthquake Network Catalogue is utilized to study local seismicity. The GA is locally seismically active such that 826 events have occurred during the period of 2005-2010, with a maximum magnitude of ML 4.24. Magnitude completeness (Mc) analysis, based on the assumption of self-similarity, suggests that all local earthquakes above a cut-off magnitude of ≥2.7 have been detected in EP. Certain basic estimates on the average depth of origin of the induced events and histogram plot on the frequency of induced and ambient (natural) seismicity are illustrated. The induced events came almost in equal proportions from the Uthmaniyah-Hawaiyah and Haradh production divisions belonging to the central and southern oil/gas Fields in GA. Poroelastic parameters of the reservoir are reviewed with respect to the induced seismicity. Focal-depth distribution of events along the strike direction of seismic zones follows the 'En-Nala axis' in the GA and is used, together with ISC data, to broadly define the seismogenic crust from a 3D-perspective. Seismic activity below both production divisions is supposedly triggered by hydrocarbon fluid-extraction; locally triggered seismicity shows better correlation to mutually opposite reverse faults transgressing the Haradh and Uthmaniyah-Hawaiyah production divisions under the influence of regional compressive stress oriented along N40°E. Results from four composite focal mechanism solutions also support this contention.

INTRODUCTION

The Jurassic intra-platform sub-basins in the EP of Saudi Arabia, together with their extension in the Arabian Gulf region are well known for their hydrocarbon occurrences. The RA formed as a result of E-W directed compression acting across EP where the axis of the anticlines is oriented in the NNW direction (Konert et al., 2001). The Qatar Arc forms the farthest limit between the central Arabian sub-basin along its western edge and the south Arabian Gulf sub-basin to its east. The compression exerted on the crust formed the regularly-spaced super-giant anticlines in EP, Bahrain, and Qatar; these are known as the RA (Sorkhabi, 2010). The Precambrian RA is bounded by the NE-trending Wadi Batin fault (WBF) and NW-trending AbuJifan fault (AJF) at its northern and southern extremities, their exact nature is obscure, but they are believed to be strike-slip faults forming part of a more widespread collision slip-line field in a framework of a microplate called the Arabian block forming the distant foreland for the Zagros (Weijarmars, 1998) (Fig.1). In this paper, the name GA has been considered as synonymous to the Ghawar fields, including the oil and gas fields developed over the GA, such that the En-Nala axis actually defines the anticlinal fold. The producing formations in GA are upper/middle Jurassic, upper/lower Permian, lower Devonian.

The GA is nearly 350 km long with an average width of about 30 km and uniform flank dips of 5-8°. There are six culminations from north to south: Farzan, Ain Dar, Shedgum, Uthmaniyah, Hawaiyah, and Haradh. The areas of structural uplift and elevation variation for three profiles across the Ghawar uplift, XX', YY' and ZZ', are illustrated in Fig.2. The GA in the south has a simple anticlinal form that extends as far north as the Huiya area, where the eastern flank shows an offset of 10-15 km before resuming the general north-south trend. The structural models proposed for the GA by Saner et al. (2005) are in broad agreement with the observations from the three topographic profiles. The surface topographic relief seen here is mostly traceable in its sub-surface, as demonstrated by the three structural sections based on seismic and well data pertaining to the three sectors of the GA between the north and south (Wender et al., 1998). The GA forms a large basement horst of Hercynian age that has been reactivated a number of times, most importantly during the late Cretaceous. However, by the Miocene, the development of the anticline was almost complete (Edgell, 1992). The GA encompasses an area of 5,308 km^2 where high oil productivity is usually associated with calc-arenitic limestone. Oil production in the GA is ~5 million B/D from the Jurassic Arab-D reservoir and gas production is 8 billion SCF/D from the Paleozoic gas reservoirs (Afifi, 2004). Well productivity generally decreases from north to south because of a reduction in reservoir thickness and a corresponding reduction in porosity and permeability (Greg Croft Inc., 1996). Oil field performance studies using ASTER satellite data for the periods of 2001 and 2007 for Shedgum and Haradh production divisions (which respectively cover 497 and 488 km^2 at the two extremities of GA) illustrate that both areas acted as 'hot spots' for oil field production activities, such as production sites and drilling rigs (Bonnet, 2015). Local earthquake data considered in the present study are for the period 2005-2010 and thus have at least some mutual overlapping period. Data analysis presented below shows that seismic activity is mainly pronounced in the Uthmaniyah, Hawaiyah, and Haradh production divisions.

The objective of the present study is to investigate the extent of crustal seismicity in the EP in relation to current deformation within the Arabian Block microplate at the Zagros foreland. This is of significance because the RA developed within this compressive tectonic active environment, and the GA seismicity is located within the RA. Next, the nature of the intense seismic zone embedded in the GA that supposedly originates from triggered seismicity related to hydrocarbon extraction is investigated. As it can be found in literature that induced

0016-7622/2018-91-4-449/$ 1.00 © GEOL. SOC. INDIA | DOI: 10.1007/s12594-018-0878-x

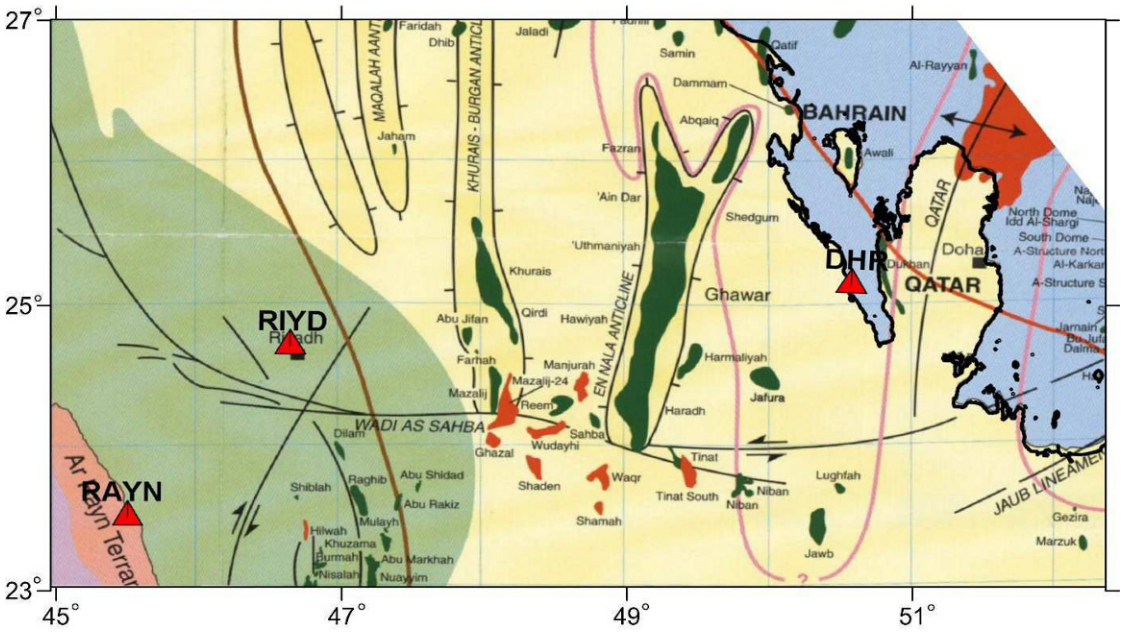

Fig.1. Plate tectonic setting of the East Arabian block in Saudi Arabia within which the Rayn anticlines developed. Their distribution from east to west: Qatar, Ghawar, Khurais-Burgan, Summan and the Amar Arc. The region experienced intense crustal deformation in the Plio-Quaternary. Modified fromWeijarmars (1998). Red triangles are seismic stations: 1, RAYN (Ar-Rayn); 2, RIYD (Riyadh); 3, DHR (Dhahran).

seismicity in oilfields are gaining ever-increasing worldwide importance due to potential in energy technologies (NRC, 2013). The present study, within its limited objectives, is accomplished by using the data from the local seismic network operated by SGS for the period of 2005-2010. First, the magnitude completeness of the data is observed in the present case. Characteristics of triggered seismicity below the Ghawar oil/gas Fields are investigated, including the "a and b-value distributions" for seismic events originating mainly from the two production divisions in GA. This allows us to draw meaningful relationships between the disposition of triggered events and locally mapped lineaments or fracture trends in the respective production divisions and brittle-ductile transition at the mid-crust.

SEISMOGENIC CRUST IN THE RAYN ANTICLINES AND INDUCED SEISMICITY IN THE GHAWAR FIELDS

Seismogenic Crust in the Eastern Province

The seismic activity status for the EP has been discussed by Al-Amri and Rodgers (2013). Elsewhere the nature of oilfield seismicity as well as crustal seismicity in areas further north of RA under the Kuwaiti Oilfields using the data from Kuwait Seismic Network has been discussed by Bou-Rabee and Mukhopadhyay (2008). Earthquake detection capability in the EP has greatly improved through the Saudi Arabian Digital Seismic Network (SANDSN),which has been installed and operated by the Saudi Geological Survey (SGS)

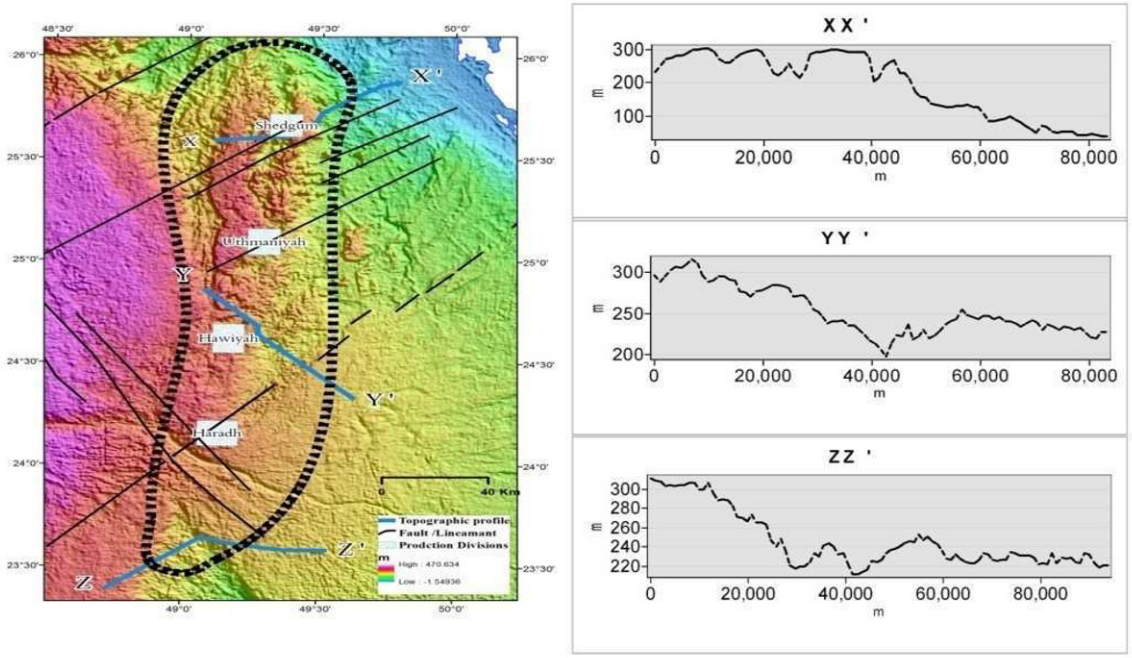

Fig.2. Digital elevation map of the Ghawar Anticline. Three topographic profiles: XX', YY' and ZZ' taken across its northern, central and southern parts illustrate the surface elevation variation.

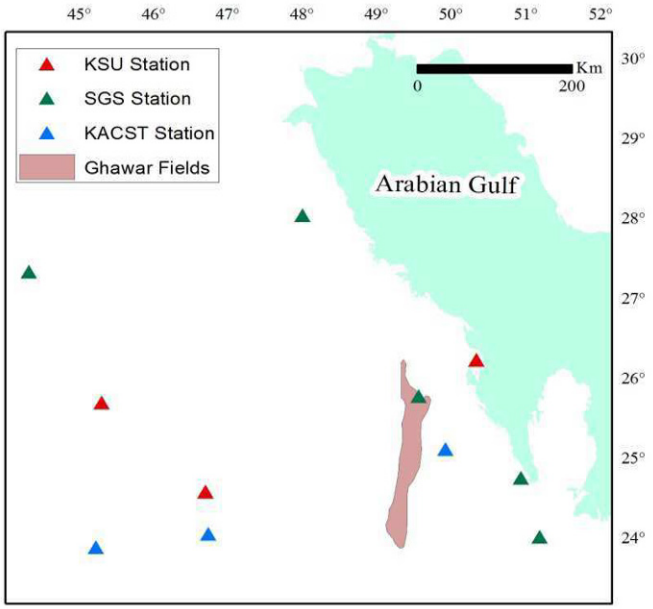

Fig.3. Local seismic network proximal to the Ghawar Fields in the Eastern Province, Saudi Arabia.

since 1998 (www.sgs.org.sa). Details of the SGS operated Seismic Network of 15 stations in the EP can be found in Endo et al. (2007) (Fig.3); available seismicity data from the SGS network corresponding to the period 2005-2010 are considered here.

To investigate the ambient seismicity of the EP, the reviewed ISC Event Catalogue was considered (International Seismological Centre 2010). In total, 21 events are listed in the catalogue corresponding to the period of 1970-2010 originated within the study area. A revised seismicity map prepared using the catalogue shows that seismic activity is largely confined between the GA and Qatar Arc as well as to the south of the AJF. Here the approximate width of the seismogenic crust is about 220 km, which is nearly six to seven times wider than the typical width of the GA. In other words, crustal seismicity is not solely restricted to the GA; rather, it encompasses a much wider expanse beneath the EP. Only a gross pattern can however be visualized here from available data from ISC bulletins. The SGS seismic network actually provides more extensive coverage on local seismicity.

Induced Seismicity in the Ghawar Fields

To distinguish between induced seismicity and natural or ambient seismicity in a tectonically complex region can often prove to be a challenging task (Dahm et al., 2013); this is more so for the region under consideration where the Arabian block microplate forms the foreland for the Zagros mountains (Weijarmars, 1998) (Fig. 1). This has resulted into a damaged crust creating basement uplift to various proportions accompanied by penetrative faulting (Edgell, 1992) and a seismogenic crust. Elsewhere an initial description on the nature of the seismogenic crust where the Rayn anticlines developed has been given (Mogren and Mukhopadhyay, 2013) but our present understanding is far too inadequate when compared to data available on the seismogenic crust for other regions, for instance, the Bohemian seismogenic massif in SE Germany where field geophysical methods are also utilized (Švancara et al., 2008). It should be realized that an unambiguous identification of any seismic event as natural or induced becomes however difficult when the seismic network data available in public domain are not exclusively dedicated to detection of the latter events alone, even though certain criteria for distinction between the injection (cause) and seismicity (affects) have been debated in literature over the years (Davis and Frohlich, 1993; Maxwell, 2013).

Available seismicity data from the SGS earthquake catalogue for the GA and its immediate adjacent areas for the period 2005-2010 demonstrate highly intense seismic activity (Fig.4). This is believed to be primarily due to regional compressive stress but also due to induced seismicity triggered by hydrocarbon extraction in the GA. It is known that induced seismicity in hydrocarbon fields usually produces small to moderate magnitude earthquake events; hence only a local network intimate to the oil/gas fields can detect such events (de Waal et al., 2015). Seismicity in oil-gas fields is often triggered by fluid-injection-induced aseismic slip (Guglielmi et al., 2015). Because of their extremely shallow depth of origin (comparable to reservoir depths), they can locally produce surface damages. For instance, a local event ML 3.6 on August 16, 2012 in Groningen gas field (Netherlands) was not seismologically intense, yet it created mapped intensities as high as VI because of the shallow depth of the event (3 km, i.e., reservoir depth) and the soft surface soils in the area (van Thienen-Visser and Breunese, 2015).

Another difficulty in studying induced seismicity in oil fields is that there may be ambient seismicity present in the region (Suckale, 2009). As discussed below, such ambient or natural seismicity in the EP may obscure the true nature of induced seismicity in GA; ambient seismicity originates from regionally operative crustal stress acting across the RA in the east-west direction. Furthermore, much valuable research on this topic has been carried out by the oil industry but is seldom made public. Consequently, any research carried out without

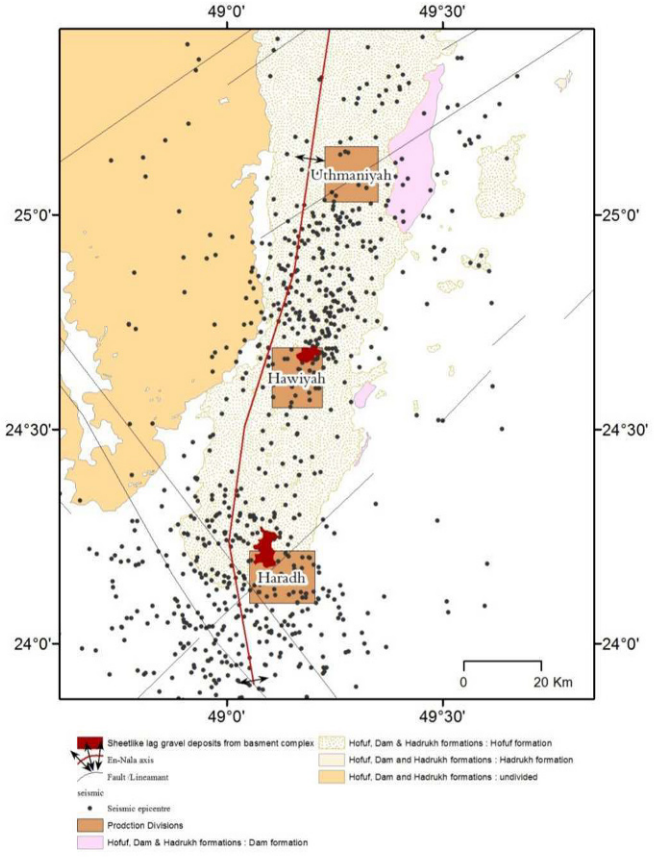

Fig.4. Spatial variation of seismic activity during 2005-2010. Seismic events are shown as black dots, are compiled based on Saudi Geological Survey Data Catalog. These events came almost in equal proportions from the two seismic zones, 49% from Uthmaniyah-Hawaiyah, and 51% from Haradh production divisions, suggesting equality in activity. Vertical movement continuing into Late Quaternary is further corroborated by the mapped 'Sheet-like Lag deposits' in the Haradh and Hawaiyah production divisions within the GA (source: Steineke et al. 1979).

the support of the oil industry is bound to remain incomplete. Notwithstanding these limitations, the analysis of local seismicity in the GA yielded some interesting results (Fig. 4). Two intense seismic zones can be distinguished from Fig.4 plot; they respectively correspond to the Uthmaniyah-Hawaiyah and Haradh production divisions of the Saudi Arabian Oil Company (ARAMCO) in the central and southern parts of the GA. In all, they produced 826 events, with a maximum magnitude of ML 4.24, during the data reporting period. These events came almost in equal proportions from the two seismic zones (49% from Uthmaniyah-Hawaiyah and 51% from Haradh production divisions), suggesting equality in activity. Seismic activity in both production divisions extends to the crustal depths and is symmetrically disposed with respect to the En-Nala anticlinal axis (Figs. 1 and 4). The along-strike orientation of the seismic zone changes from NE to NNE between the two production divisions with diminished activity. Significant variation is noticeable in the sub-surface configuration between the along-strike and orthogonal disposition of the event depths, which are discussed elsewhere. This is, however, subject to the level of certainty to which the event depths are determined by the existing SGS seismic network.

Magnitude Completeness in the Saudi Geological Survey Earthquake Data Catalogue for the Eastern Province

It has long been recognized that both monitoring and earthquake detection accuracy are equally significant in discriminating between induced and ambient or natural events. Both qualitative criteria and quantitative formulation are used to discriminate whether an event is anthropogenic or natural and whether it is triggered or induced? Dahm et al. (2013) propose a combination of probabilistic influence diagrams (similar to volcano hazard analysis) as an aid for discrimination. The readers are also referred to the following recent research advances because of their political and scientific discussion: (a) global review of human-induced earthquakes, prepared by U.K. Group (Foulger et al., 2013), (b) Australian examples on triggered earthquakes for developing a path towards quantification of earthquake hazards (Gibson and Sandiford, 2013) and (c) USGS review on injection-induced earthquakes and earthquake hazard in USA (Ellsworth, 2013, Petersen et al., 2016). Whether there is only ambient (natural) seismicity or induced activity or their combination, it is useful to assess the magnitude of completeness (Mc) in any earthquake catalog that is to be used for analysis for a given region. Simplest definition of Mc is the lowest magnitude at which 100% earthquakes, both spatial and temporal, are detectable using the given instrumental set up in a region. Mignan and Woessner (2012) have discussed several issues relating to the correct use of Mc and explained why the correct determination of Mc is not a trivial task.

The SGS data catalogue for the period 2005-2010 available for the present study area contains as many as 826 events with magnitude (ML) ranging from 0.17 to 4.24. To determine Mc in the SGS catalogue, a methodology based on the assumption of self-similarity was adopted (Wiemer and Wyss 2000). A fast and reliable estimate of Mc by this method is used to define the point of the maximum curvature (MAXC) as the 'magnitude of completeness,' which is done by computing the maximum value of the first derivative of the frequency-magnitude curve. In practice, this aligns with the magnitude bin with the highest frequency of events in the non-cumulative frequency-magnitude distribution. The highest frequency of events in the non-cumulative data curve has a flat peak at magnitude of 2.7 for the highest frequency class, which by definition can be taken as the Mc (Fig.5). Here, the Gutenberg-Richter relation: log (cumulative frequency) – magnitude illustrates that for magnitude 2.7 and above, the curve is smooth and follows a straight line, thereby implying that all earthquakes in the region that are monitored and catalogued by the SGS earthquake Network are by and large monitored above this cut-off magnitude of

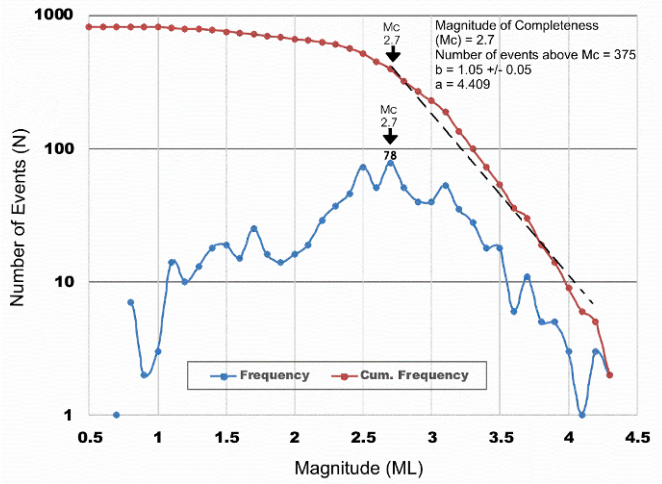

Fig.5. Magnitude completeness Mc≥2.7 as determined for SGS Earthquake catalogue. Refer text for discussion.

≥2.7.The total number of events above and equal to Mc is 375 which yields b-value 1.05± 0.05 and a-value 4.409 calculated by maximum likelihood method of Aki (1965). This value on Mc however differs from that given by Zahran et al. (2013) who, by making use of the frequency-magnitude histogram, infer that most events greater than magnitude 1 have been located for the area by the existing network.

b-Value Estimates

The b-value calculated by the maximum likelihood method (Aki, 1965) is 1.05±0.05 with a-value 4.409 (Fig.5) as described in the last section. This moderate b-value is indicative of locally induced activity proximal to the reservoir source zone, presumably having high asperity. Based on the available data, it was found that the highest magnitude expected locally (a/b) is 4.12. This agrees well with the highest locally monitored magnitude (ML 4.2) by the SGS network thus far. Statistically, a higher magnitude event of ML 5.15 in coming 10 years can be expected. However, improved estimates of the highest probable earthquake magnitude for induced events can be obtained only with a denser seismic network for the GA. Such example is found in Groningen gas field in Netherlands where induced or triggered seismicity in hydrocarbon fields are closely monitored through much closer local network facilities (Muntendam-Bos and de Waal, 2013).

Induced Seismicity in the Ghawar Anticline: Poroelastic Considerations

A reservoir is a porous and permeable lithological unit or a set of units that holds hydrocarbon reserves. It has long been recognized that pore pressure change is the primary cause of reservoir-induced seismicity; such variation in pore pressure actually gets transmitted to seismic focal depths through diffusion (Talwani and Acree, 1984). Seismicity associated with pore pressure diffusion occurs in crusts with seismogenic permeability, *k*s, of ~2 to 200 mD (Talwani, 2000). Triggered seismicity of the Ghawar oil/gas reservoirs at the simplest level requires, therefore, an assessment of their porosity and permeability. Porosity and permeability estimations for the Ghawar Fields have been reported by many since the early stage of its exploration, including Saner and Sahin (1999), Lucia et al. (2002) and Sahin et al. (2007). Both average porosity and permeability estimates for the oil producing Arab-D reservoir in the Ghawar field are known to vary significantly from south to north (Fig. 4 and Table 1; data source: Greg Croft Inc. 1996, based on Saudi Aramco data in 1980). Average porosity ranges between 14 and 19%, showing a gradual increase from south to north. Average permeability (*k*) in the

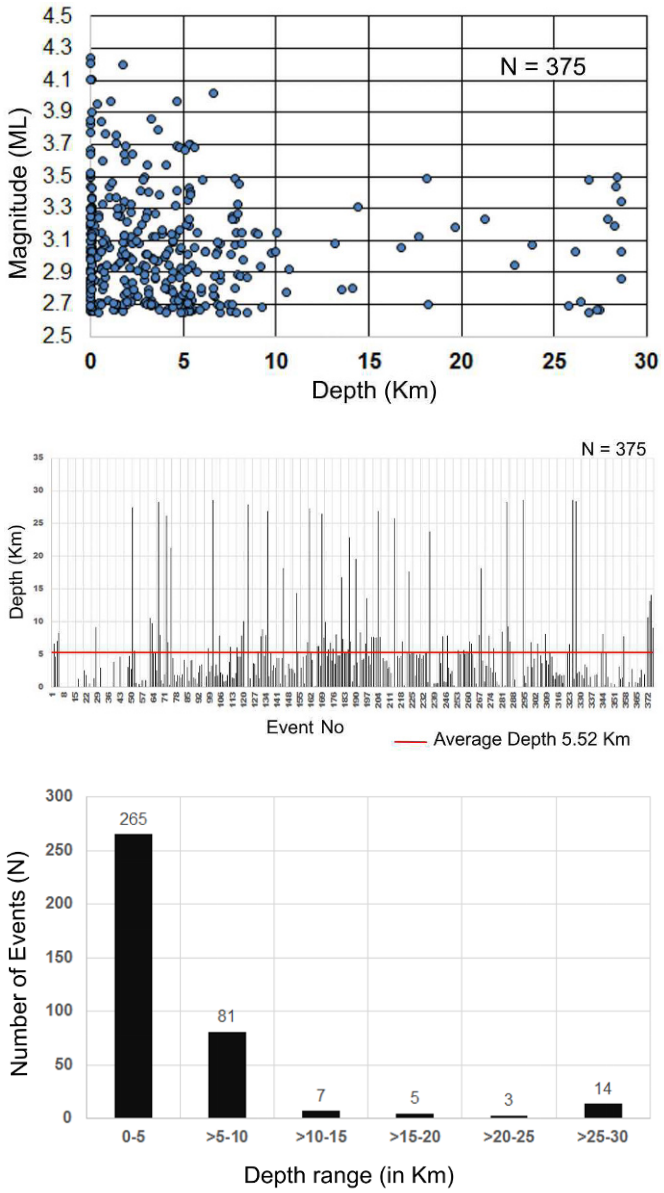

Fig.6. (a) Plot showing the events magnitude versus depth; total number of events is 375 above Mc. Note that the majority of events locate within about 5 km in upper crust, **(b)** Plot showing events (375 above Mc) with depth; average depth of origin is 5.52 km, **(c)** Bar diagram of events with depth. Most events (265 out of 375) were produced from about 5 km depth in top crust.

Arab-D reservoir exhibits an increase by as much as four times between the Haradh (av. = 52 mD) and the Uthmaniyah production divisions (av. = 220 mD); to more than one order higher to Ain Dar Area (= 617 mD). However, so large an increase in intrinsic permeability creates no distinct discriminating influence on triggered seismicity in the top overburden, where the local seismicity is clearly equally intensive and crust-penetrative between the Haradh and Uthmaniyah Production Divisions (refer the foregoing section). This is probably because the seismic activity below both production divisions is more a result of the combined factors of regional stress and hydrocarbon extraction-induced activity rather than solely due to any single parameter. The effect of intrinsic permeability on induced seismicity has been discussed by many regarding reservoir-induced areas and other hydrocarbon fields in the world (Ingebritsen and Manning, 2010). Usually two factors are considered to govern the situation: poroelastic coupling between pore pressure and the earthquake nucleation which is time-dependent. Seagall and Lu (2015) suggest that for constant injection rate, the required time to reach the critical seismicity rate is given by $t = r^2/(cf_c)$, where r = distance from the injector, c = hydraulic diffusivity and fc is a factor dependent more on mechanical properties of rocks but also weakly on r. It is speculated that the deep-penetrative faults continuing from the thick sediments into the basement along the margins of GA and also within it (Edgell, 1992; Wender et al., 1998) clearly play a very significant role by responding to such poroelastic properties in consequence to fluid injection to overlying strata. Here the permeability of the fault zone is considered significant for the hydraulic connectivity between the fault and the target sediment horizon. Most likely that high seismicity rates would exhibit affinity on permeable and hydraulically connected faults due to direct pore pressure diffusion, while the lower seismicity rates are predicted on isolated normal faults originating due to steeper normal faults (Chang and Segall, 2016). Although further discussion on this topic is beyond the purview of the present study, yet a brief reference in the following section on the nature of faulting derived from composite fault plane solutions for seismic events under GA is made.

Table 1. Poroelastic parameters for the Arab-D Reservoir, Ghawar Oilfields (source: GregCroft 1996)

Reservoir parameters at different areas	Net Thickness (m)	Porosity (%)	Permeability (mD)	Productivity Index (BOPD/PSI)
Ain Dar Area	62	19	617	141
Shedgum Area	59	19	639	141
Uthmaniyah Area	55	18	220	92
Hawaiyah Area	55	17	68	45
Haradh Area	43	14	52	31

Surface deformation in Induced Seismic Zones in the Ghawar Fields – Composite Focal Mechanism Solutions

Stress measurements within hydrocarbon reservoirs show that the least horizontal stress decreases with declining reservoir pressure, as predicted by poroelasticity. The observed faulting associated with fluid withdrawal is known to vary for the upper and lower horizons of a reservoir; normal faults develop on the flanks of the field when the depleted reservoir is located in an extensional environment, whereas reverse faults develop above and below the reservoir in compressive environments (cf. Segall and Fitzgerald, 1998). For circular disk-shaped reservoirs, isothermal reduction in pore pressure induces a relative horizontal tension within the reservoir. Production-induced stress may promote frictional sliding along pre-existing faults. Within the reservoir itself, normal faulting is promoted if the regional stress is extensional and the Biot coefficient is sufficiently large, alpha >0.85, for reasonable coefficients of friction. On the other hand, dilatation fracturing and normal faulting are always promoted in extensional environments near the edge of the reservoir or in regions with a high pore-pressure gradient. It is suggested that such fracturing could enhance the fracture permeability in tight rocks adjacent to portions of the reservoir that experience large reductions in pore pressure because of production. In regional compressive environments, production modestly favors reverse faulting above and below the reservoir, which appears to be the situation in the present case. Some support for this inference is provided by the gross results based on composite focal mechanism solutions for the southern areas of the GA. Composite focal mechanism solutions for the localized seismic events identified in four areas at the south end of the GA (after Al-Shamrani, 2007) are schematically illustrated in Fig.8. This allows us to infer the faulting pattern at depth and correlate it to mapped lineaments/faults on the surface where the identified areas, 1 through 4, are criss crossed by a set of lineaments/faults running NW and NE, which parallel the AJF and WBF, respectively (Fig. 1). Composite

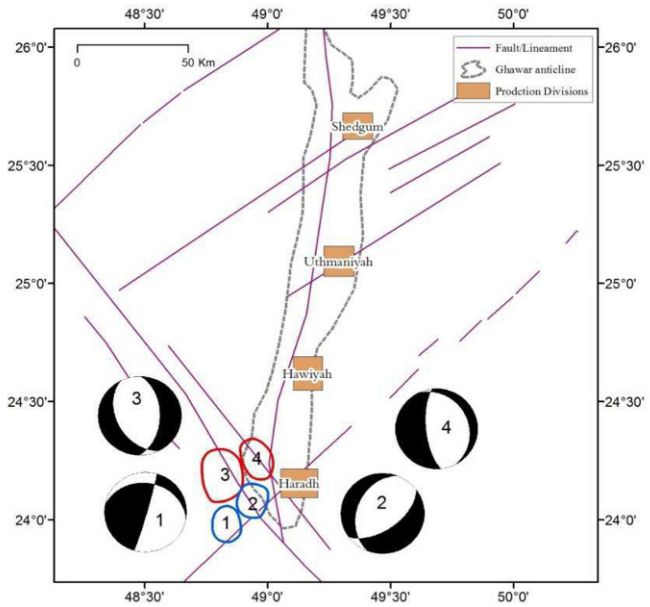

Fig.7. Composite focal mechanism solutions for the four identified local earthquakes at the southern end of the Ghawar Field (after Al-Shamrani, 2007). Refer text for discussion.

focal mechanism plots illustrate that normal faulting is the dominant pattern, with a minor strike-slip component along the NE and NW oriented fault planes in their respective locales. Assuming that the mapped surface lineaments/faults also represent faults at depth, the NNE-NE oriented focal planes in solutions 1 and 2 and the NW focal-planes in solutions 3 and 4 are considered to be the fault planes in their respective areas using this correlation. In other words, motion along northeasterly faults is left-lateral, whereas the motion changes to right-lateral for northwesterly faults. If the inferred slip motion along the crisscross faults present in the GA is extendable to their parallel master faults, the WBF should have a component of left-lateral shear, while right-lateral shear should be surmised for the AJF; the RA are dissected by both of these master faults (refer Fig. 1).The faulting pattern shown in Fig.7 is found to be largely applicable for areas corresponding to the Uthmaniyah-Hawaiyah and Haradh production divisions, where NNE and NNW oriented lineaments and fractures respectively correspond to such reverse faults in the overlying layers of the reservoir.

DISCUSSION

Triggered seismicity and subsidence in major oil and gas fields is ascribed to compaction that directly relates to depletion of oil/gas. Most often, such induced seismicity correlates to stress changes. For example, the induced seismicity of the Groningen Gas Reservoir relates to compaction that results in stress changes involving many faults in the reservoir (Muntendam Bos, et al., 2015, van Thienen- Visser and Breunese, 2015). Induced seismicity in the GA is demonstrated by mapped surface lineaments and fracture patterns for seismic zones A and B, which correspond to the Uthmaniyah-Hawaiyah and Haradh production divisions. Presumably such production-induced stress promotes frictional sliding along such basement faults. Structural uplift in the GA and its bounding faults seemingly plays an important role in influencing the current seismicity, at least in the upper crust (~15 km); this is illustrated by the 3D block diagram (Fig.8). Vertical movement continuing into the late Quaternary is further corroborated by the mapped 'Sheet-like Lag deposits' in the Haradh and Hawaiyah production divisions within the GA (Fig. 4; Steineke et al., 1979; also refer Bartholomew et al., 2002); areas of neotectonic uplift are also the areas of present-day intense seismicity. The probable geometric configuration at depth for the uplifted crustal block is inferred by gravity modeling; this generally corresponds to the pattern of near-surface uplifts mapped by seismic surveys and well data from Saudi Aramco (Wender et al., 1998; Elawadi and Mukhopadhyay, 2017).

The crust below the EP, where the AJF truncates the RA, is seismically active (as determined from the 'Reviewed International Seismological Centre (U.K.) Bulletin' data for the period 1970-2010). The EP seismogenic crust is about 110 km wide and up to 15 km thick. This estimated width is found to be substantially wider than the typical width of the GA (~30 km). The seismogenic crust evidently extends on either side of the GA, encompassing a wider rhombic zone. This is possibly an outcome of compression stress acting regionally along N40°E across the En-Nala axis, rather than being exclusively related to hydrocarbon extraction from the Ghawar Fields as popularly believed. Triggered seismicity in the Ghawar Fields is highly intense; it mainly originates from the two production divisions: the Uthmaniyah-Hawaiyah and Haradh divisions, located in the central and southern parts of the Ghawar Field, respectively. Seismic zones in the two production divisions are distributed symmetrically with respect to the En-Nala anticline axis. Vertical movement continuing into the Late Quaternary is further corroborated by the mapped 'Sheet-like Lag deposits' in the Haradh and Hawaiyah production divisions within the GA (refer to the previous section and Fig. 4); areas of Neotectonic uplift are also the areas of present-day intense seismicity.

While the microseismically active zone under GA is guided by inherited structures in the basement geology, the ambient seismicity originating at the bottom of the upper crust at ~15 km depth (Fig. 8)

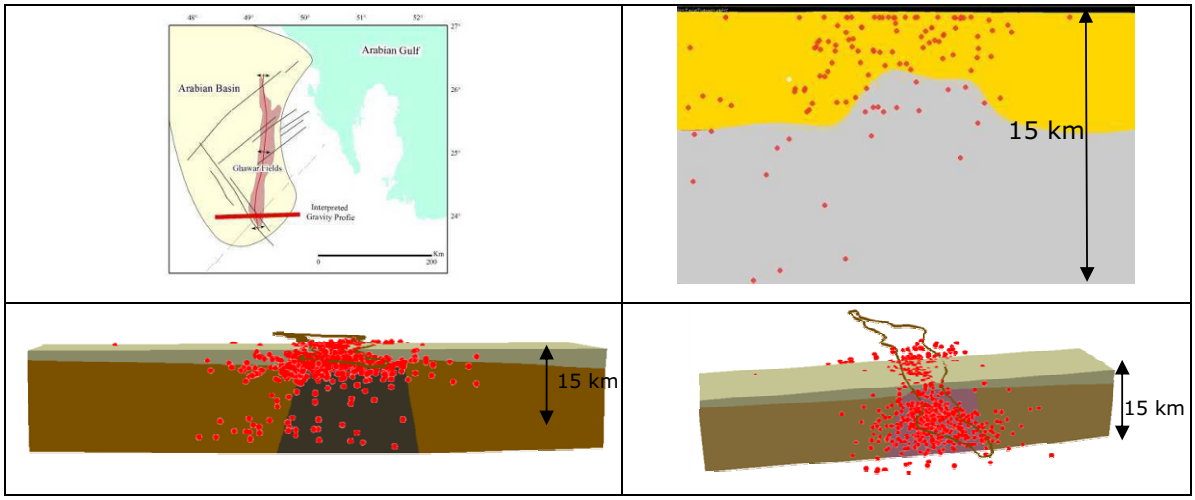

Fig.8. Block diagram showing 3D perspective for seismogenic crust under the Ghawar Anticline and its surroundings.

roughly corresponds to the brittle-ductile transition zone in a continental crust. Usually the larger earthquakes tend to nucleate near the base of the seismogenic zone (Sibson, 1982). By definition, the transition zone extends from 13-18 km depth as known from other continental regions where prevailing temperature supposedly exceeds 250°C and the rocks are less likely to fracture, rather more likely to show ductile deformation through creep (Smit et al., 2015). We conjecture that below the GA, the mid-crustal zone at ~15 km extending to somewhat deeper level acts as the strongest part of the crust where the ambient seismicity has developed in the present situation.

CONCLUSIONS

The main conclusions derived from this study are as follows:

a Analysis based on the assumption of self-similarity shows that the SGS seismic network has locally detected all earthquakes in the EP above a cut off magnitude of ≥2.7. This measure of Mc is estimated using the SGS data available for the period of 2005-2010.

b Frequency-magnitude relationships for locally monitored 826 earthquakes and their corresponding 'a and b-values' over a magnitude of ≥2.7 are provided for the first time. Triggered earthquakes occurred almost in equal proportions from beneath the two southernmost production divisions in the Ghawar fields. Such a feature is noticeable despite the fact that the intrinsic permeability in the Arab-D reservoir increases northward by as much as four times from the Haradh to the Uthmaniyah-Hawaiyah production divisions. One probable explanation for this is that triggered seismicity percolates to deeper levels, such as towards the crystalline basement or still deeper.

c It is recommended that the initial results regarding the GA presented here should be improved by using dense local seismic network datafor a larger time period. Equally important is input from the oil/gas industry to constrain the poroelastic data on seismogenic crust under the EP and the crust-penetrative nature of faults.

Acknowledgement: We are thankful to Mr. Mussed S. Al-Harbi, Seismology Division, Saudi Geological Survey, Jeddah for providing us with the seismicity data for the Eastern Province. M.M. is thankful to the Vice-Rectorate of Graduate Studies and Research, International Scientific Partnership Program, King Saud University, Riyadh, for necessary support.

References

Afifi, A.M. (2004) Ghawar: The anatomy of the world's largest oil field. Saudi Aramco.www.searchanddiscovery.com/documents

Aki, K. (1965) Maximum likelihood estimate of b in the formula log N =a–bM and its confidence limits. Bull. Earthquake Res. Inst., Univ Tokyo, v.43, pp.237–239

Al-Amri, A.M. and Rodgers, A.J. (2013) Improvement of seismicity parameters in the Arabian Shield and Platform using earthquake location and magnitude calibration. *In:* K. Al Hosani et al. (Eds.), Lithosphere Dynamics and Sedimentary Basins: The Arabian Plate and Analogues, Frontiers in Earth Sciences, Springer-Verlag Heidelberg, Chapter 14.

Al-Shamrani, A.B.S. (2007) Micro-Seismicity of Al-Ghawar Oil Field Eastern Saudi Arabia. Master's Thesis, Dept. Geology, King Saud University, Riyadh, Saudi Arabia.

Bartholomew, M.J., Stickney, M.C., Wilde, E.M. and Dundas, R.G. (2002) Late Quaternary paleoseismites: Syndepositional features and section restoration used to indicate paleoseismicity and stress-field orientations during faulting along the main Lima Reservoir Fault, southwestern Montana. *In:* F.R. Ettensohn, N. Rast, C.E. Brett, (Eds.), Ancient Seismites. Geol. Soc. Amer., Special Paper, no.359, pp.29-47.

Bonnet, A.D. (2015) Oilfield performance – Ghawar Oilfield (Saudi Arabia). GeoVille, www.geoville.com

Bou-Rabee, F. and Mukhopadhyay, M. (2008) Oilfield seismicity in Kuwait and its environmental impact. *In:* Near-surface Geophysics and Human Activity. Proc. 3rd Internat. Conf. Environ. Engg. Geophys., June 2008, Wuhan, China, Science Press, U.S.A.

Chang, K.W. and Segall, P. (2016) Injection-induced seismicity on basement faults including poroelastic stressing. Jour. Geophys. Res., Solid Earth, v.121, doi:10.1002/2015JB012561.

Dahm, T., Hainzl, S., Becker, D. and the FKPE Group DINSeis. (2013) How to discriminate induced, triggered and natural seismicity.European Center for Geodynamics & Seismology, Luxembourg, Proc. Workshop Induced Seismicity, v.30, Nov.15-17, 2010.

Davis, S.D. and Frohlich, C. (1993) Did (or will) fluid injection cause earthquakes? Criteria for a rational assessment. Seism. Res. Lett., v.64, pp.207-224.

de Waal, J.A., Muntendam-Bos, A.G. and Roest, J.P.A. (2015) Production induced subsidence and seismicity in the Groningen gas field – can it be managed? Proc. IAHS, v.372, pp.129–139. doi:10.5194/piahs-372-129-2015

Edgell, H.S. (1992) Basement tectonics of Saudi Arabia as related to oilfield structures. *In:* Richards, M., et al. (Eds.), Basement Tectonics, Kluwer Acad. Publishers, pp.169-193.

Elawadi, E. and Mukhopadhyay, M. (2017) Subsurface configuration of the Rayn Anticlines and evidences for plate margin kinematics in the East Arabian Block, Saudi Arabia – Reinterpreted results from potential field data. (submitted)

Endo, E., Zahran, H., Nofal, H. and Hadidy, S. (2007) The Saudi National Seismic Network. Seismo. Res. Lett., v.78(4), pp.439-445.

Foulger, G.R., Wilson, M., Gluyas, J., Julian, B.R. and Davies, R. (2015) A global review of human-induced earthquakes. Community.dur.ac.uk/g.r.foulger/FTP/Human Induced Earthquakes_ Durham.pdf, pp. 292.

GEOEXPRO (2010) The application of microseismics in the Oil and Gas Industry. Ghawar, Saudi Arabia: The King of Giant Fields. GeoExpro.com, v.7(4), pp.58-63.

Gibson, G. and Sandiford, M. (2013) Seismicity and induced earthquakes. Background paper to NSW Chief Scientist and Engineer (OCSE). Univ. Melbourne, pp.33.

Greg Croft Inc.(1996) TheGhawar Oil Field, Saudi Arabia. http://www.gregcroft.com/ghawar.ivnu

Guglielmi, Y., Cappa, F., Avouac, J-P., Henry, P. and Elsworth, D. (2015) Seismicity triggered by fluid injection–induced aseismic slip. Science, v.348(6240), pp.1224-1226.

Ingebritsen, S.E. and Manning, C.E. (2010) Permeability of the continental crust: dynamic variations inferred from seismicity and metamorphism. Geofluids, v.10, pp.193-205.

International Seismological Centre, On-line Bulletin, http://www.isc.ac.uk, Internat. Seis. Centre, Thatcham, United Kingdom. (2010)

Konert, G., Afifi, A.M., Al-Hazri, S.A. and Droste, H.J. (2001) Paleozoic stratigraphy and hydrocarbon habitat of the Arabian Plate. GeoArabia, v.6(3), pp.407-442.

Langenbruch, C. and Zoback, M.D. (2016) How will induced seismicity in Oklahoma respond to decreased saltwater injection rates? Science Advances, 2: e1601542, pp. 1-9.

Lucia, F.J., Jennings, J.W. and Rahnis, M. (2002) Permeability and rock fabric from wireline logs, Arab-D reservoir, Ghawar Field, Saudi Arabia. GeoArabia, v.6(4), pp.619-646.

Maxwell, S. (2013) Unintentional seismicity induced by hydraulic fracturing. FOCUS Article, Schlumberger, CSEG Recorder, pp.40-49.

Mignan, A. and Woessner, J. (2012) Estimating the magnitude of completeness in earthquake catalogs. Community Online Resource for Statistical Seismicity Analysis. doi:10.5078/corssa-00180805.

Mogren, S. and Mukhopadhyay, M. (2013) Study of seismogenic crust in the Eastern Province of Saudi Arabia and its relation to the seismicity of the Ghawar Fields. Abstract, Am. Geophys. Union, Fall Meeting, 9-13 Dec.

Muntendam-Bos, A. G. and de Waal, J.A. (2013) Reassessment of the probability of higher magnitude earthquakes in the Groningen gas field: SodM technical report, http://www. sodm.nl/sites/default/files/redactie/rapport%20analyse%20 aardbevingsgegevens%20 groningse% 20gasveld %2016012013

National Research Council, (2013) Induced Seismicity Potential in Energy Technologies, Washington, D.C.: The National Academies Press. doi:10.17226/13355, pp.262.

Petersen, M.D., Mueller, C.S., Moschetti, M.P., Hoover, S.M., Llenos, A.L.,

Ellsworth, W.L., Michael, A.J., Rubenstein, J.L., McGarr, A.F. and Rukstales, K.S. (2016) Seismic-hazard forecast for 2016 including induced and natural earthquakes in the Central and Eastern United States. Seism. Res. Lett., v.87(6), pp.1327-1341. Doi:10.1785/0220160072

Sagar, S. and Leonard, M. (2008) Mapping the magnitude of completeness of the Australian earthquake catalogue. Publn. Geoscience Australia, pp.8.

Sahin, A., Ali, A.Z., Saner, S. and Menouar, H. (2007) Permeability anisotropy distributions in an Upper Jurassic carbonate reservoir, Eastern Saudi Arabia. Jour. Pet. Geol., v.30(2), pp.147-158.

Saner, S. and Sahin, A. (1999) Lithological and zonal porosity-permeability distributions in the Arab-D reservoir, Uthmaniyah Field, Saudi Arabia. AAPG Bull., v.83(2), pp.230-243.

Saner, S., Al-Hinai, K. and Perincek, D. (2005) Surface expression of the Ghawarstructure, Saudi Arabia. Marine Pet. Geol., v.22, pp.657-670.

Saudi Geological Survey Jeddah. National Centre for Earthquakes and Volcanoes. www.sgs.org.sa

Švancara, J., Havir, J. and Conrad, W.(2008) Derived gravity field of the seismogenic upper crust of SE Germany and West Bohemia and its comparison with seismicity. Stud. Geophys. Geod., v.52, pp.567-588.

Segall, P. and Fitzgerald, S.D. (1998) A note on induced stress changes in hydrocarbon and geothermal reservoirs. Tectonophys., v.289, pp.117-128.

Segall, P. and Lu, S. (2015) Injection-induced seismicity: Poroelastic and earthquake nucleation effects. Jour. Geophys. Res., Solid Earth, v.120: 5082-5103. doi:10.1002/2015/B012060

Sibson, R.H. (1982) Fault zone models, heat flow and the depth distribution of earthquakes in the continental crust of the United States. Bull. Seismol. Soc. Amer., v.72(1), pp.151-163.

Smit, L., Fagerenga, A., Braeuer, B. and Stankiewicz, J. (2015) Microseismic activity and basement controls on an active intraplate strike-slip fault, Ceres-Tulbagh, South Africa. Bull. Seismol. Soc. Amer., v.105, pp.1540-1547.

Sorkhabi, R. (2010) The King of Giant Fields. GEO Expro, v.4(7). http://www.geoexpro.com

Steineke, M., Harriss, T.F., Parsons, K.R. and Berg, E.L. (1979) Geologic map of the Western Arabian Gulf Quadrangle, Kingdom of Saudi Arabia. Geologic Map GM-208 A. Min. Pet. Min. Res., Dir. Gen. Min. Res., Jeddah, Saudi Arabia.

Suckale, J. (2009) Induced seismicity in hydrocarbon fields. Advances in Geophysics, v.51, Chapter 2, pp.1-52.

Talwani, P. (2000) Seismogenic properties of the crust inferred from recent studies of reservoir induced seismicity – Application to Koyna. Curr. Sci., v.79(9), pp.1327-1333.

Talwani, P. and Acree, S. (1984) Pore pressure diffusion and the mechanism of reservoir induced seismicity. PAGEOPH, v.122.

vanThienen-Visser, K. and Breunese, J.N. (2015) Induced seismicity of the Groningen gas field: History and recent developments. The Leading Edge, Special Section: Injection-induced Seismicity, June 2015, pp.664-671.

Weijarmars, R. (1998) Plio-Quaternary movement of the East Arabian Block. GeoArabia, v.3(4), pp.509-540.

Wender, L.E., Bryant, J.W., Dickens, M.F., Neville, A.S. and Al-Moqbel, A.M. (1998) Paleozoic (pre-Khuff) hydrocarbon geology of the Ghawar area, eastern Saudi Arabia. GeoArabia, v.3, pp.273-302.

Wiemer, S. and Wyss, M. (2000) Minimum magnitude of completeness in earthquake catalogs: examples from Alaska, the Western United States, and Japan. Bull. Seismol. Soc. Amer., v.90, pp.859-869.

Zahran, H.M., El_hadidy, S. and Yosef, K. (2010) Recent earthquake activity at Haradh region, Western Saudi Arabia. European Center for Geodynamics & Seismology, Luxembourg, Proc. Workshop Induced Seismicity, v.30, Nov. 15-17, 2010.

(Received: 22 September 2016; Revised form accepted: 23 August 2017)